Upregulation of p16^{INK4A} in Peripheral White Blood Cells as a Novel Screening Marker for Colorectal Carcinoma

Running title: p16^{INK4A} in WBCs of CRC

Khin Aye Thin[1], Phonthep Angsuwatcharakon[2], Steven W Edwards[3], Apiwat Mutirangura[2, 4], Charoenchai Puttipanyalears[2,4*]

[1]Joint PhD Program in Biomedical Sciences and Biotechnology between Faculty of Medicine, Chulalongkorn University, Bangkok, 10330, Thailand and Institute of Integrative Biology, University of Liverpool, Liverpool, L7 8TX, United Kingdom.

[2]Department of Anatomy, Faculty of Medicine, Chulalongkorn University, Bangkok, 10330, Thailand.

[3]Institute of Infection, Veterinary and Ecological Sciences, University of Liverpool, Liverpool, L7 8TX, United Kingdom.

[4]Center of Excellence in Molecular Genetics of Cancer and Human Diseases, Department of Anatomy, Faculty of Medicine, Chulalongkorn University, Bangkok, 10330, Thailand.

***Corresponding author:**

Dr. Charoenchai Puttipanyalears, Ph.D.

Department of Anatomy, Faculty of Medicine, Chulalongkorn University, 1873 Rama IV Road, Pathumwan, Bangkok, 10330 Thailand

+662-256-4281#1713

charoenchai.p@chula.ac.th

ABSTRACT

Objective: Screening of colorectal cancer (CRC) is important for the early detection. CRC is relating to aging and immuno-senescence. One such senescent marker is $p16^{INK4A}$ expression in immune cells. The objective of the study is to investigate the protein expression of $p16^{INK4A}$ in peripheral white blood cells as a screening marker for colorectal cancer.

Methods: A case-control studies were conducted. Cases were patients with colorectal cancer and controls were matched with cases based on age and sex. Peripheral blood was collected from patients and controls and measured for the protein $p16^{INK4A}$ with immunofluorescent techniques. The $p16^{INK4A}$ levels from cases and controls were evaluated using ROC analysis to be used as a screening marker in CRC patients. Mean fluorescent intensity of $p16^{INK4A}$ of cases and controls were analyzed in CD45+, CD3+ or CD14+ cells. The $p16^{INK4A}$ levels of cases were also correlated with clinical data.

Result: Statistically significant increased expression of $p16^{INK4A}$ levels were found in cases compared to controls. $p16^{INK4A}$ in peripheral immune cells had 78% sensitivity and 71% specificity which can possibly be used as a diagnosis tool for colorectal cancer. $P16^{INK4A}$-positive cell percentage and mean florescent intensity were significantly higher in CD45 positive cells, CD3 positive cells and CD14 positive cells. No significant correlation was observed with the clinical data and $p16^{INK4A}$ level of CRC patients.

Conclusion: The significant increase of $p16^{INK4A}$ expression level in peripheral immune cells represents potential for use as a CRC screening marker.

Keywords: $p16^{INK4A}$, immune cells, colorectal carcinoma, Immunofluorescence

INTRODUCTION

Colorectal cancer (CRC) is the third most common cancer and second highest leading cause of cancer deaths worldwide (Inadomi and Jung, 2020), accounting for about 10% of cancer incidence and 9.4% of cancer deaths around the world in 2020 (Xi and Xu, 2021). Disease incidence can vary with sex, age, geographical regions and lifestyles differences, where higher incidence has been reported in males than in females and is higher in more-developed regions than in less-developed regions (Rawla et al., 2019). The majority of CRC patients have sporadic diseases with no family history of CRC, while about 5% to 10% of CRC cases are hereditary (Rawla et al., 2019).

CRC is more common in aging population. Most sporadic CRC patients are >50 years of age, with about 75% of rectal cancer patients and 80% of colon cancer patients diagnosed in their 60s and above (Kuipers et al., 2015). Aging relates to the colonic epithelial proliferation (Roncucci et al., 1988; Holt et al., 2009), epigenetic alterations and genomic instability (Mutirangura, 2019). The other important thing is the collective changes of the immune system, termed as immuno-senescence, can also be seen with age (Xu et al., 2020). Although immune responses may inhibit cancer growth, they can also stimulate cancer growth and metastasis, as a consequence of immuno-senescence (Pawelec, 2017) and tumor-associated inflammation (Grizzi et al., 2013). One of the aging markers is $p16^{INK4A}$.

$p16^{INK4A}$ is a cell cycle regulator, functioning as a cyclin-dependent kinase inhibitor of the INK4 family (Laphanuwat and Jirawatnotai, 2019) and tumor suppressor protein (Buj and Aird, 2019). It in its canonical pathway (RB pathway) can act as an aging marker (LaPak and Burd, 2014). Increased expression of $p16^{INK4A}$ is observed in pathophysiological conditions such as tumorigenesis and senescence (Liu et al., 2009). Therefore, it is worth to elucidate $p16^{INK4A}$ in

CRC patients' immune cells as a marker. This research aimed to measure the protein expression of $p16^{INK4A}$ in peripheral white blood cell of CRC patients for application as a diagnostic tool. Then, we investigated the CD3+ cells represented T lymphocytes and CD14+ cells represented monocytes to find whether or not they manifest the $p16^{INK4A}$ protein.

MATERIALS AND METHODS

Study design and target population

Cross-sectional case-control studies were done at the King Chulalongkorn Memorial Hospital. All samples were collected from May 2021 to December 2021. Control samples were collected from patients without a family history of cancer, autoimmune diseases and showed negative CRC screening results from colonoscopy. This group served as normal controls for this study. Sample size was calculated from the pilot study using the formula $N = 2(Z\alpha/2 + Z\beta)^2 * \sigma^2 / (\bar{X}_1-\bar{X}_2)^2$ with α significance level at 0.05 and power β of 90%, which required at least 53 participants in each group. Colorectal cancer staging was assessed by the American Joint Committee on Cancer TNM system by a pathologist. Venous whole blood (2 mL) with anticoagulant EDTA was collected from participant based on WHO guidelines.

$p16^{INK4A}$ Assay

Difference in $p16^{INK4A}$ clones can affect the outcomes of the experiments (Sawicka et al., 2013; Shain et al., 2018). Therefore, we validate the $p16^{INK4A}$ antibodies with cell lines: Hela (American Type Culture Collection: ATCC® CCL-2™), HCT116 (American Type Culture Collection: ATCC® CCL-247™), and keratinocytes. Antibodies to $p16^{INK4A}$ (cell signaling) were rabbit monoclonal antibodies. D3W8G (92803) was raised against synthetic peptide residues surrounding Ala34 of human $p16^{INK4A}$ protein. D7CM1(80772) was produced from the synthetic

peptide residues surrounding Ala143 of human $p16^{INK4A}$ protein. D3W8G and D7CM1 antibodies showed positive staining stain in Hela cells (Fig 1A and 1B). D7CM1 antibodies had strong cytoplasmic staining in keratinocytes (Fig 1C). D3W8G antibodies showed nuclear staining in keratinocytes (Fig 1D). Hct116 cells were used as negative control for $p16^{INK4A}$ staining (Fig 1E and 1F) (Myöhänen et al., 1998). Cytoplasmic $p16^{INK4A}$ could have various functions other than its canonical function of cell cycle regulation and senescence (Buj and Aird, 2019). Therefore, we focused on the D3W8G antibodies.

Buffy coat layer preparation

Whole blood was centrifuged at 1000g for 12 min at room temperature. The buffy coat layer was collected, and the red blood cells (RBCs) were lysed with 20 volumes of RBC lysis solution (Abcam, USA). The lysis reaction was terminated by adding an equal volume of phosphate buffered saline (PBS) and centrifuged for 5 min at 400g. Cells were washed with PBS 3 times and white blood cells (WBCs) were counted with a counting chamber. WBCs were then fixed with 4% paraformaldehyde for 15 min (1 million cells/mL fixative) and washed 3 times with deionized water. WBCs were placed in 96-well plates (approximately 40,000 cells/ well) and stored at room temperature before immuno-fluorescence staining.

Immunofluorescence staining

Sample wells containing WBCs were washed with PBS 3 times. One hundred microliter of 0.5% Triton X-100 was added into each well and incubated for 10 min at room temperature. Wells were then washed with PBS 5 times. Then, 100µl of 5% (w/v) BSA was added into each well for 30 min. One hundred µL of diluted primary antibodies (anti-$p16^{INK4A}$ and anti-CD45) in 1% (w/v) BSA, were added into each well and incubated overnight (16 h) at 4°C. Dilutions of

anti-$p16^{INK4A}$ primary rabbit antibody (Cell Signaling) and anti-CD45 primary mouse antibody (Abcam) were 1:1000. Anti-CD3 primary mouse antibody (Cell signaling) and anti-CD14 primary mouse antibody (Cell signaling) were diluted 1:500. Wells were washed with 100 µL of 0.1% Tween PBS 3 times. One hundred µL of 1:1000 diluted secondary fluorescent antibodies (anti-rabbit FITC and anti-mouse Cy3) (cell signaling) in 1% (w/v) BSA, were added into each well and incubated for 2 h at room temperature in the dark. Wells were washed with PBS 3 times. One hundred µL of DAPI (final concentration of 1µg/ml) (for nuclear staining) was added into each well for 10 min and washed with PBS for 3 times.

Image analysis

Three-color images were captured as follows: blue (DAPI 358 - 461 nm); green (FITC 500 - 520 nm) and red (Cy3 560 - 570 nm) with a motorized fluorescence microscope IX83 (Olympus Co., Ltd., USA). All images were acquired using a defined experimental protocol throughout the study. Briefly, 20 fields of 20X objective (5 columns and 5 rows) were taken with the fixed exposure time for DAPI (7s), FITC (200ms) and Cy3 (300ms). The fluorescence intensity of cell was calculated using CellSens imaging software after setting the range of intensity values (70 to 150) and perimeter values (18 to 55 nm). Mean fluorescence intensity (MFI) was then acquired from the average fluorescence intensity of cells from the whole image. In double immunofluorescence staining, the positive region was identified by using CancerScreen.exe program (Puttipanyalears et al., 2021). $P16^{INK4A}$-positive/ CD-positive cells were identified by the signals of red and green in the same spot with the criteria of intensity value (60 to 150) and perimeter value (18-100 nm).

Ethical approval

This study was conducted under the regulations of the Institutional Review Board, Faculty of Medicine, Chulalongkorn University, COA number: 1580/2021. This study was conducted in accordance with the Declaration of Helsinki. All study participants provided informed consent.

Statistical analysis

Normal distribution values of the study groups were assessed by Shapiro-wilk test. To detect the significant differences of measurements between CRC and healthy control participants, independent sample t-tests was used. For comparison between more than two groups, ANOVA was calculated. Data are expressed as mean±SD, 95% CI and p-value. Receiver operating characteristic (ROC) curve and Youden index were used to evaluate the sensitivity and specificity of the marker. GraphPad prism-8 (GraphPad Software Inc., USA) was used for statistical analysis and graphical illustrations.

RESULTS

I. $p16^{INK4A}$ protein level in white blood cells of cases and controls

$p16^{INK4A}$ levels were measured in the peripheral white blood cells of CRC patients (Fig 2A) and normal controls. Since $p16^{INK4A}$ levels can depend on donor age, the normal control was age- and sex-matched to the CRC cohort. Comparison of cases with controls revealed a statistically significant increase in MFI per cell between CRC patients compared to controls (Fig 2B) (95% CI = 2.8 to 11.9, p = 0.003).

Then, we increased the number of samples both in CRC and control, not adjusted by age and sex. The total number of CRC patients in this study was 72 with mean age of 64.54±11.3 years, while that of healthy controls was 79 with a mean age of 63.91±8.8 years. Cases and controls demographics are shown in Table 1. The minimum age of study participants was 31 years and maximum age was 89 years. The values in samples were normally distributed according to Shapiro-Wilk test. Therefore, we calculated the difference of the two groups with the independent sample t-test. Among the total number of CRC 72 and control 79, there was also a statistically significant increase MFI of $p16^{INK4A}$ in WBC of CRC patients compared to controls (Fig 2C) (95% CI = 4.5 to 8.3, $p<0.001$).

II. Evaluation of $p16^{INK4A}$ as a marker in CRC patients

$p16^{INK4A}$ levels in peripheral immune cells were observed to be used as a marker in CRC patients, as the $p16^{INK4A}$ level of peripheral white blood cells increased in CRC patients compared to controls. ROC curve was calculated using MFI of $p16^{INK4A}$ in CD45+ cells of patients and control. Area under the curve was 78% ($p <0.001$) with the standard error value of 0.04. There was 78% sensitivity and 71% specificity with Youden index of 0.48, cut-off value of 83.26 MFI (Fig 3). From 2x2 table, true positive (TP) number for CRC is 56, false negative (FN) number for CRC is 16, false positive (FP) number for normal control is 23 and true negative (TN) number for normal control is 56. Therefore, sensitivity (TP/TP+FN) is 78%, specificity (TN/FP+TN) is 71%, positive predictive value (TP/TP+FP) is 71%, negative predictive value (TN/FN+TN) is 78% and accuracy (TP+TN / TP+FP+FN+TN) is 74%.

III. $p16^{INK4A}$ expression according to clinical data of CRC patients

$p16^{INK4A}$ protein levels in CRC samples were analyzed based on clinical parameters such as the stages of CRC, tumor size, lymph node involvement, metastasis status, patients age and histological types of tumors (Fig 4 A-F). Of the 72 patients from CRC group, clinical data of 2 patients were not available, resulting their exclusion from the analysis. CRC samples were categorized based on the age as <50-year, 50-64 year, and 65 and above year. Half of patients (55.6%) were in the population of 65 and above. There is no significant difference of $p16^{INK4A}$ level among the age groups ($F(2, 69) = 0.4$, $p = 0.7$). Regarding to gender, 62.5% of patients in the study were male and showed higher MFI of $p16^{INK4A}$, but no statistically significant difference ($t=1.3$, $p=0.2$). When the $p16^{INK4A}$ levels were observed according to the stages, size and lymph node involvement of tumors, their levels were similar, showing the statistical values of stage ($F(3, 66) = 0.1$, $p = 0.9$), tumor size ($F(3, 66) = 0.3$, $p = 0.8$) and lymph node involvement ($F(3, 66) = 0.2$, $p = 0.8$). Thirty percent of patients had metastasis, and their $p16^{INK4A}$ MFI were not statistically different from that of non-metastasis patients ($t = 0.5$, $p = 0.6$). Clinical data of CRC patients were shown in Table 1.

IV. Expression of $p16^{INK4A}$ in peripheral blood CD45+ cells, CD3+ cells and CD14+ cells of cases and controls

We used double immunofluorescence staining to investigate lymphocytes and monocytes positive for $p16^{INK4A}$. Antibodies of $p16^{INK4A}$ and CD3 were used to detect $p16^{INK4A}$-positive lymphocytes (Fig 5A). For monocytes population, antibodies of $p16^{INK4A}$ and CD14 were used (Fig 5B). Mean fluorescence intensity of $p16^{INK4A}$ in CD3+ cells and CD14+ cells were calculated in CRC patients and normal controls. A significant increase in levels of $p16^{INK4A}$ were

observed in CD3+ cells (95% CI = 0.2 to 9.1, p = 0.04) and CD14+ cells (95% CI = 0.2 to 6.3, p = 0.04) of CRC patients. Expression of $p16^{INK4A}$ was higher in CD3+ cells than in CD14+ cells. (95% CI = 0.4 to 6.6, p = 0.03) (Fig 5C).

The number of $p16^{INK4A}$-positive white blood cells increased in CRC patients, revealing a significant difference in CD45+ subset (95% CI = 3.2 to 24.3, p = 0.01), in CD3+ subset (95% CI = 0.06 to 17.1, p = 0.05) and in CD14+ subset (95% CI = 1.0 to 13.2, p = 0.02) (Fig 6A). When the number of $p16^{INK4A}$ positive cells and MFI of each cell subset were combined in a graph, there were increasing trend of higher value in $p16^{INK4A}$ and percent positive cells in CRC groups (Fig 6B, 6C and 6D).

DISCUSSION

With immunofluorescence technique, we can measure the intensity of the positive cells and number of positive cells. The MFI of $p16^{INK4A}$ in WBC of CRC patients had a significantly higher value than that of healthy control group in this study. $P16^{INK4A}$ in peripheral immune cells represents 78% sensitivity and 71% specificity for application as a potential colorectal cancer screening marker. Proteins, DNA, RNA and metabolites from tissue, blood, stool and urine have been used in CRC for screening, diagnosis and monitoring, but have varying degree of success to be used as an effective biomarker (Loktionov, 2020). Colonoscopy has been used as the gold standard for the diagnosis of CRC (Hazewinkel and Dekker, 2011). Blood-based protein biomarkers for detection of CRC have various sensitivity and specificity, while using protein panel increase the detection rate of CRC (Loktionov, 2020).

The increased expressions of $p16^{INK4A}$ have been notified in the peripheral blood cells of testicular cancer survivors (Bourlon et al., 2020) and breast cancer survivors (Sanoff et al.,

2014). Presence of $p16^{INK4A}$ in the immune cells can represent immuno-senescence (Liu et al., 2009). Immuno-senescence is initiated earlier in men than in women, likely due to hormonal differences between males and females, as estrogen enhances immune responses, while progesterone and androgens favor immune suppressive actions (Ostan et al., 2016). Therefore, we investigated age and sex-adjusted CRC patients and controls, the MFI in CRC group is significantly higher, meaning that immuno-senescence can contribute to CRC patients regardless of age and sex. Immuno-senescence can result from oxidative stress, cellular and DNA damage, chronic inflammation and cytotoxic therapy (De Padova et al., 2021). According to Giunco, *et al*, immuno-senescence in CRC patients can lead to negative consequences like disease relapse, progression and death (Giunco et al., 2019).

CRC group showed increased $p16^{INK4A}$ levels compared to normal controls. However, stages of CRC were not correlated to the level of $p16^{INK4A}$ which is similar to the finding of Milde-Langosch, *et al* that reported $p16^{INK4A}$ expression was not correlated with the clinical stages of breast cancer (Milde-Langosch et al., 2001). MFI value of $p16^{INK4A}$ were higher in some categories and was found to be relatively high in the categories of late stage, male patients and old age, but there were no statistically significant differences**.** The immune landscape in elderly population and metastasis patients differ from other patients in both innate and adaptive immune system (Weng, 2006; Fulop et al., 2017; Blomberg et al., 2018). The various factors can influence the level of $p16^{INK4A}$ in immune cells, as $p16^{INK4A}$ has an impact on immune surveillance (Sznurkowski et al., 2017; Leon et al., 2021). Limitations of this study include the small sample size (n) of some categories and due to the nature of this cross-sectional study, we could not prove that $p16^{INK4A}$ level correlates to the prognosis of the patients.

Protein expression of $p16^{INK4A}$ was higher in T cell subsets of CRC patients. T cells are important for tumor immunity and immunotherapy (Woolaver et al., 2021). Senescent T cells relate to progression of cancers (Vicente et al., 2016). Senescent T cells in CRC patients also relate to patient negative outcomes such as disease relapse, disease progression and death (Giunco et al., 2019). $p16^{INK4A}$ expression in peripheral blood T cells is associated with chronologic age, molecular age, and IL-6 production (Liu et al., 2009; Burd et al., 2020). IL-6 is important in human frailty (Soysal et al., 2016) and relates to cellular senescence (Kojima et al., 2013). $p16^{INK4A}$ protein expression increase in T cells of peripheral blood and bone marrow of acute lymphoblastic leukemia and its expression correlates to senescent features (Chebel et al., 2007).

Monocytes also expressed $p16^{INK4A}$ protein in CRC patients in this study. Monocytes are a heterogenous group of cells. A typical portion (about 85%) of monocytes are classical monocytes ($CD14^{high}$ $CD16^{-}$), the rest (5 to 10 % each) are intermediate monocytes ($CD14^{+}$ $CD16^{+}$) and non-classical monocytes ($CD14^{dim}$ $CD16^{high}$) (Coillard and Segura, 2019; Kapellos et al., 2019). Monocyte recruitment to the inflammation sites and cancer tissue is an important process and it can occur within hours of onset of inflammation (Coillard and Segura, 2019). Moreover, monocytes can be transformed into monocyte-derived macrophages (Mo-mac) and monocyte-derived dendritic cells (mo-DC) (Coillard and Segura, 2019). On the other side, $p16^{INK4A}$ can stimulate the maturation of mo-DC through MAPK pathway (Sunthamala et al., 2020). Mo-DC can be found especially in the intestines (Watchmaker et al., 2014). In addition, $p16^{INK4A}$ can involve in macrophage polarization (Cudejko et al., 2011; Kuo et al., 2011; Hall et al., 2017).

CONCLUSION

The well-known aging marker $p16^{INK4A}$ in peripheral blood of CRC patients has been observed in this study. The statistically significant increase of $p16^{INK4A}$ level in WBCs revealed a potential diagnostic tool for CRC. However, the protein expressions of $p16^{INK4A}$ were divergent with CRC patients' clinical data. Functions of $p16^{INK4A}$ in CRC patient immune cells are interesting topics that warrant further studies.

Author's contributions

The experiments were conducted and designed by CP and AM. The clinical samples were collected by KAT, PA and CP. KAT and CP performed and optimized the immunofluorescent staining. The results were analyzed and interpreted by KAT, CP and AM. KAT wrote the manuscript. CP, SWE and AM reviewed and edited the manuscript. All authors read and approved the final manuscript.

Conflicts of interest statement

Every author in this study has completed an International Committee of Medical Journal Editors Form for Uniform Disclosure of Potential Conflicts of Interest. The authors declare that they have no competing interests.

Abbreviation

ATCC American Type Culture Collection

CRC Colorectal cancer

MFI Mean fluorescence intensity

PBS Phosphate buffer saline

RBC Red blood cell

ROC Receiver operating characteristic

WBC White blood cell

REFERENCES

Blomberg OS, Spagnuolo L, de Visser KE (2018). Immune regulation of metastasis: mechanistic insights and therapeutic opportunities. *Dis Model Mech,* **11**.

Bourlon MT, Velazquez HE, Hinojosa J, et al (2020). Immunosenescence profile and expression of the aging biomarker (p16INK4a) in testicular cancer survivors treated with chemotherapy. *BMC Cancer,* **20,** 882.

Buj R, Aird K (2019). p16: cycling off the beaten path. *Molecular & Cellular Oncology,* **6,** 1677140.

Burd CE, Peng J, Laskowski BF, et al (2020). Association of Epigenetic Age and p16INK4a With Markers of T-Cell Composition in a Healthy Cohort. *J Gerontol A Biol Sci Med Sci,* **75,** 2299-303.

Chebel A, Chien WW, Gerland LM, et al (2007). Does p16ink4a expression increase with the number of cell doublings in normal and malignant lymphocytes? *Leuk Res,* **31,** 1649-58.

Coillard A, Segura E (2019). In vivo Differentiation of Human Monocytes. *Frontiers in Immunology,* **10**.

Cudejko C, Wouters K, Fuentes L, et al (2011). p16INK4a deficiency promotes IL-4-induced polarization and inhibits proinflammatory signaling in macrophages. *Blood,* **118,** 2556-66.

De Padova S, Urbini M, Schepisi G, et al (2021). Immunosenescence in Testicular Cancer Survivors: Potential Implications of Cancer Therapies and Psychological Distress. *Frontiers in oncology,* **10,** 564346-.

Fulop T, Larbi A, Dupuis G, et al (2017). Immunosenescence and Inflamm-Aging As Two Sides of the Same Coin: Friends or Foes? *Front Immunol,* **8,** 1960.

Giunco S, Petrara MR, Bergamo F, et al (2019). Immune senescence and immune activation in elderly colorectal cancer patients. *Aging,* **11,** 3864-75.

Grizzi F, Bianchi P, Malesci A, et al (2013). Prognostic value of innate and adaptive immunity in colorectal cancer. *World journal of gastroenterology,* **19,** 174-84.

Hall BM, Balan V, Gleiberman AS, et al (2017). p16(Ink4a) and senescence-associated β-galactosidase can be induced in macrophages as part of a reversible response to physiological stimuli. *Aging (Albany NY),* **9,** 1867-84.

Hazewinkel Y, Dekker E (2011). Colonoscopy: basic principles and novel techniques. *Nat Rev Gastroenterol Hepatol,* **8,** 554-64.

Holt PR, Kozuch P, Mewar S (2009). Colon cancer and the elderly: from screening to treatment in management of GI disease in the elderly. *Best practice & research. Clinical gastroenterology,* **23,** 889-907.

Inadomi J, Jung B (2020). Colorectal Cancer—Recent Advances and Future Challenges. *Gastroenterology,* **158,** 289-90.

Kapellos TS, Bonaguro L, Gemünd I, et al (2019). Human Monocyte Subsets and Phenotypes in Major Chronic Inflammatory Diseases. *Frontiers in Immunology,* **10**.

Kojima H, Inoue T, Kunimoto H, et al (2013). IL-6-STAT3 signaling and premature senescence. *JAK-STAT,* **2,** e25763-e.

Kuipers EJ, Grady WM, Lieberman D, et al (2015). Colorectal cancer. *Nature Reviews Disease Primers,* **1,** 15065.

Kuo CL, Murphy AJ, Sayers S, et al (2011). Cdkn2a is an atherosclerosis modifier locus that regulates monocyte/macrophage proliferation. *Arterioscler Thromb Vasc Biol,* **31,** 2483-92.

LaPak KM, Burd CE (2014). The molecular balancing act of p16(INK4a) in cancer and aging. *Mol Cancer Res,* **12,** 167-83.

Laphanuwat P, Jirawatnotai S (2019). Immunomodulatory Roles of Cell Cycle Regulators. *Frontiers in Cell and Developmental Biology,* **7**.

Leon KE, Tangudu NK, Aird KM, et al (2021). Loss of p16: A Bouncer of the Immunological Surveillance? *Life (Basel),* **11**.

Liu Y, Sanoff HK, Cho H, et al (2009). Expression of p16(INK4a) in peripheral blood T-cells is a biomarker of human aging. *Aging cell,* **8,** 439-48.

Loktionov A (2020). Biomarkers for detecting colorectal cancer non-invasively: DNA, RNA or proteins? *World journal of gastrointestinal oncology,* **12,** 124-48.

Milde-Langosch K, Bamberger AM, Rieck G, et al (2001). Overexpression of the p16 cell cycle inhibitor in breast cancer is associated with a more malignant phenotype. *Breast Cancer Res Treat,* **67,** 61-70.

Mutirangura A (2019). A Hypothesis to Explain How the DNA of Elderly People Is Prone to Damage: Genome-Wide Hypomethylation Drives Genomic Instability in the Elderly by Reducing Youth-Associated Gnome-Stabilizing DNA Gaps. In 'Epigenetics', Eds IntecOpen, 65-75

Myöhänen SK, Baylin SB, Herman JG (1998). Hypermethylation can selectively silence individual p16ink4A alleles in neoplasia. *Cancer Res,* **58,** 591-3.

Ostan R, Monti D, Gueresi P, et al (2016). Gender, aging and longevity in humans: an update of an intriguing/neglected scenario paving the way to a gender-specific medicine. *Clinical science (London, England : 1979),* **130,** 1711-25.

Pawelec G (2017). Immunosenescence and cancer. *Biogerontology,* **18,** 717-21.

Puttipanyalears C, Denariyakoon S, Angsuwatcharakon P, et al (2021). Quantitative STAU2 measurement in lymphocytes for breast cancer risk assessment. *Scientific Reports,* **11,** 915.

Rawla P, Sunkara T, Barsouk A (2019). Epidemiology of colorectal cancer: incidence, mortality, survival, and risk factors. *Przeglad gastroenterologiczny,* **14,** 89-103.

Roncucci L, Ponz de Leon M, Scalmati A, et al (1988). The influence of age on colonic epithelial cell proliferation. *Cancer,* **62,** 2373-7.

Sanoff HK, Deal AM, Krishnamurthy J, et al (2014). Effect of cytotoxic chemotherapy on markers of molecular age in patients with breast cancer. *J Natl Cancer Inst,* **106,** dju057.

Sawicka M, Pawlikowski J, Wilson S, et al (2013). The Specificity and Patterns of Staining in Human Cells and Tissues of p16INK4a Antibodies Demonstrate Variant Antigen Binding. *PLOS ONE,* **8,** e53313.

Shain AF, Wilbur DC, Stoler MH, et al (2018). Test Characteristics of Specific p16 Clones in the Detection of High-grade Squamous Intraepithelial Lesions (HSIL). *International Journal of Gynecological Pathology,* **37**.

Soysal P, Stubbs B, Lucato P, et al (2016). Inflammation and frailty in the elderly: A systematic review and meta-analysis. *Ageing Research Reviews,* **31,** 1-8.

Sunthamala N, Sankla N, Chuerduangphui J, et al (2020). Enhancement of specific T-lymphocyte responses by monocyte-derived dendritic cells pulsed with E2 protein of human papillomavirus 16 and human p16INK4A. *PeerJ,* **8,** e9213.

Sznurkowski JJ, Żawrocki A, Biernat W (2017). Local immune response depends on p16 INK4a status of primary tumor in vulvar squamous cell carcinoma. *Oncotarget,* **8**.

Vicente R, Mausset-Bonnefont AL, Jorgensen C, et al (2016). Cellular senescence impact on immune cell fate and function. *Aging Cell,* **15,** 400-6.

Watchmaker PB, Lahl K, Lee M, et al (2014). Comparative transcriptional and functional profiling defines conserved programs of intestinal DC differentiation in humans and mice. *Nat Immunol,* **15,** 98-108.

Weng NP (2006). Aging of the immune system: how much can the adaptive immune system adapt? *Immunity,* **24,** 495-9.

Woolaver RA, Wang X, Krinsky AL, et al (2021). Differences in TCR repertoire and T cell activation underlie the divergent outcomes of antitumor immune responses in tumor-eradicating versus tumor-progressing hosts. *Journal for ImmunoTherapy of Cancer,* **9,** e001615.

Xi Y, Xu P (2021). Global colorectal cancer burden in 2020 and projections to 2040. *Translational Oncology,* **14,** 101174.

Xu W, Wong G, Hwang YY, et al (2020). The untwining of immunosenescence and aging. *Semin Immunopathol,* **42,** 559-72.

Acknowledgements

We would like to thank Department of Anatomy, Chulalongkorn University for equipment and Center of Excellence in Molecular Genetics of Cancer and Human Diseases, Faculty of Medicine, Chulalongkorn University for specimen collection. This research project was financially supported by Office of the Permanent Secretary, Ministry of Higher Education, Science, Research and Innovation (Grant number RGNS 63-004) and the funding source of Graduate Scholarship Program for ASEAN and Non-ASEAN Countries. The study was

approved by the Institutional Review Board, Faculty of Medicine, Chulalongkorn University, with the COA number: 1580/2021 as part of the thesis. The authors declared no conflict of interest. The authors' contribution to the paper is as follow: study design and conception: CP, AM; data collection: KAT, PA, CP; data analysis and interpretation: KAT, CP, AM; manuscript preparation: KAT; review and editing: SWE, AM.

Table

Table (1) Cases and Controls demographics and clinical criteria of CRC patients

Parameters	N	%	Elderly population for each category (Age 65 and above) N (%)
Age (range) of Normal Controls			
<50	3	3.8	0
50-64	39	49.4	0
65 and above	37	46.8	37 (100)
Gender of Normal Controls			
Male	31	39.2	16 (51.6)
Female	48	60.8	21 (43.8)
Age (range) of CRCs			
<50	5	6.9	0
50-64	27	37.5	0
65 and above	40	55.6	40 (100)

Gender of CRCs			
Male	45	62.5	24 (53.3)
Female	27	37.5	16 (59.3)
Stages of CRCs			
I	6	8.6	3 (50.0)
II	17	24.3	13 (76.5)
III	26	37.1	12 (46.2)
IV	21	30.0	10 (47.6)
Tumor size of CRCs			
T1	4	5.7	2 (50)
T2	8	11.4	5 (62.5)
T3	42	60.0	22 (52.4)
T4	16	22.9	9 (56.3)
Lymph node involvement of CRCs			
N0	29	41.4	19 (65.5)
N1	29	41.4	15 (51.7)
N2	12	17.1	4 (33.3)
Metastasis status of CRCs			
Metastasis	21	30.0	11 (52.4)
Non metastasis	49	70.0	27 (55.1)

Tumor histological types of CRCs			
Well differentiated adenocarcinoma	14	20.0	8 (57.1)
Moderately differentiated adenocarcinoma	47	67.1	24 (51.1)
Poorly differentiated adenocarcinoma	1	1.4	1 (100)
Epithelioid cell carcinoma	1	1.4	0
Mucinous adenocarcinoma	5	7.1	4 (80)
Signet ring cell carcinoma	2	2.9	1 (50)
Left or right-side tumor of CRCs			
Left side	62	88.6	32 (51.6)
Right side	8	11.4	6 (75.0)
Tumor location of CRCs			
Cecum	2	2.9	2 (100.0)
Ascending colon	4	5.7	3 (75.0)
Hepatic flexure	1	1.4	0
Transverse colon	1	1.4	1 (100.0)
Descending colon	5	7.1	5 (100.0)
Sigmoid colon	12	17.1	7 (58.3)
Recto-sigmoid colon	2	2.9	1 (50.0)
Rectum	43	61.4	19 (44.2)

Figures

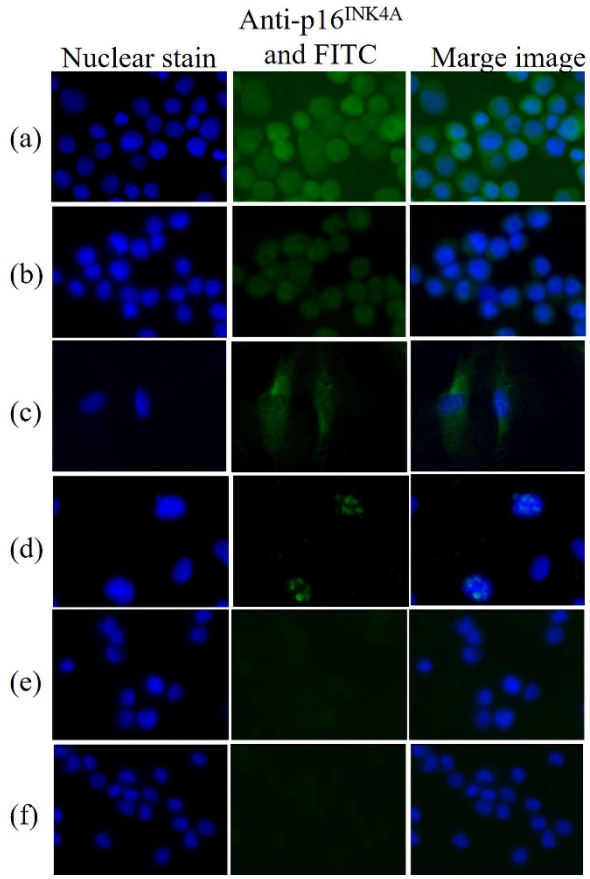

Fig (1)

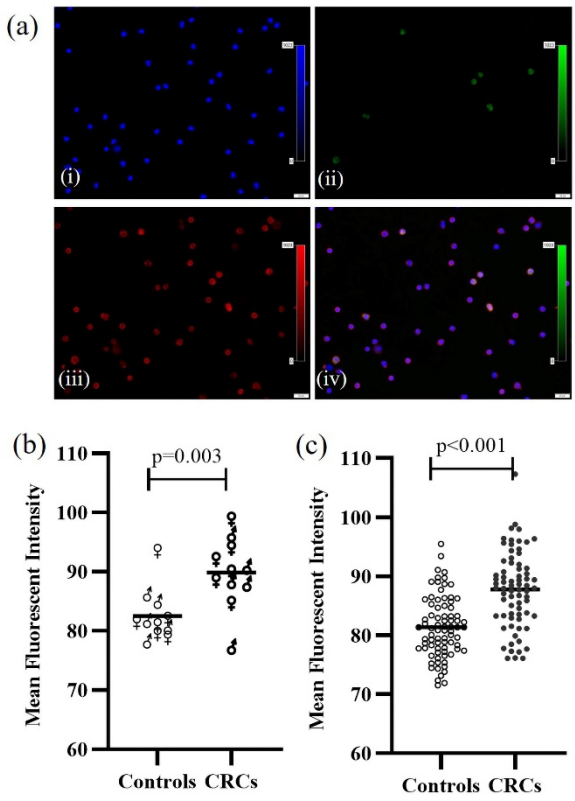
(a)
(i)
(ii)
(iii)
(iv)
(b)
p=0.003
Mean Fluorescent Intensity
110
100
90
80
70
60
Controls CRCs
(c)
p<0.001
Mean Fluorescent Intensity
110
100
90
80
70
60
Controls CRCs

Fig (2)

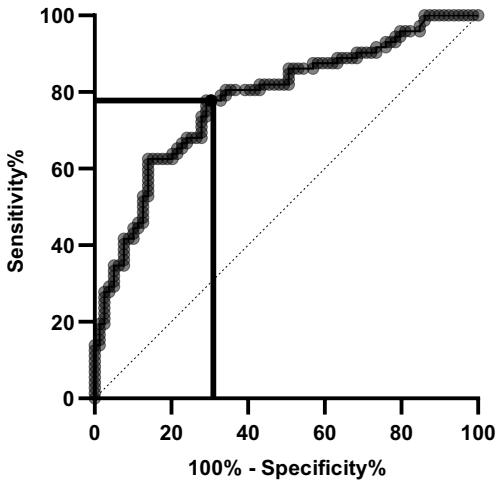

Fig (3)

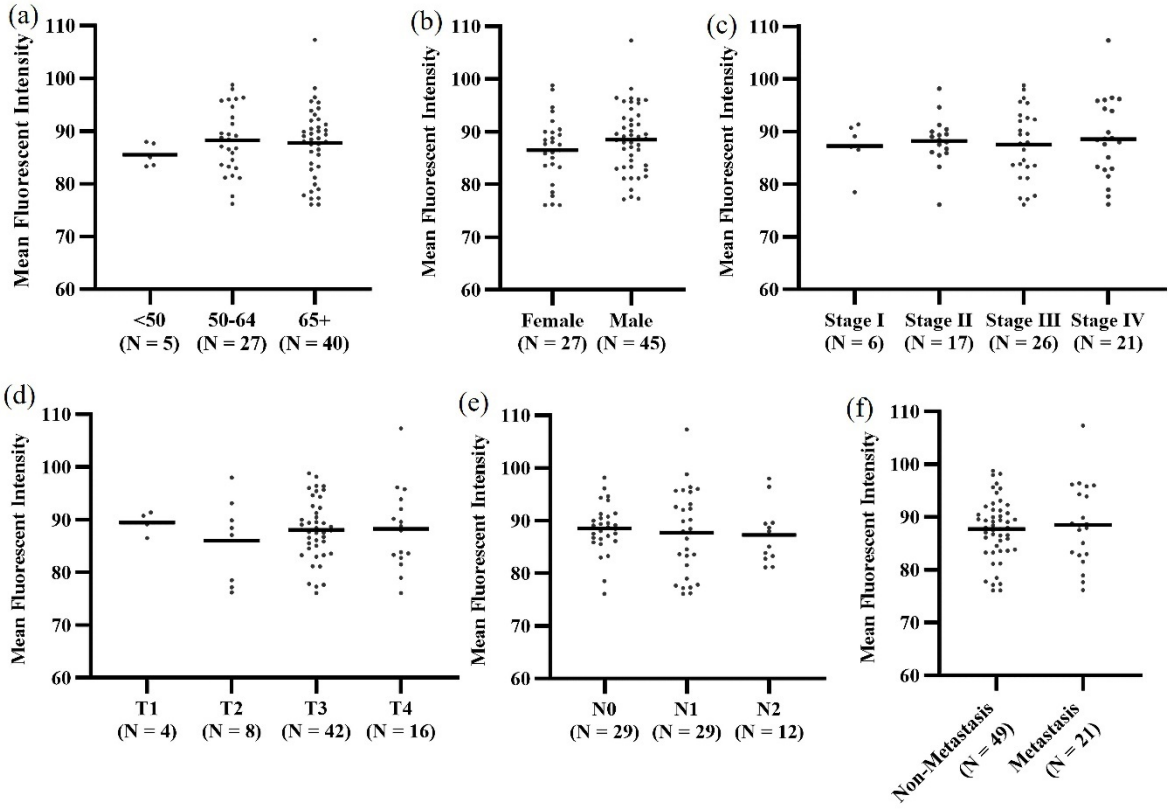
(a)
Mean Fluorescent Intensity
110
100
90
80
70
60
<50 (N = 5)
50-64 (N = 27)
65+ (N = 40)
(b)
Mean Fluorescent Intensity
Female (N = 27)
Male (N = 45)
(c)
Mean Fluorescent Intensity
Stage I (N = 6)
Stage II (N = 17)
Stage III (N = 26)
Stage IV (N = 21)
(d)
Mean Fluorescent Intensity
T1 (N = 4)
T2 (N = 8)
T3 (N = 42)
T4 (N = 16)
(e)
Mean Fluorescent Intensity
N0 (N = 29)
N1 (N = 29)
N2 (N = 12)
(f)
Mean Fluorescent Intensity
Non-Metastasis (N = 49)
Metastasis (N = 21)

Fig (4)

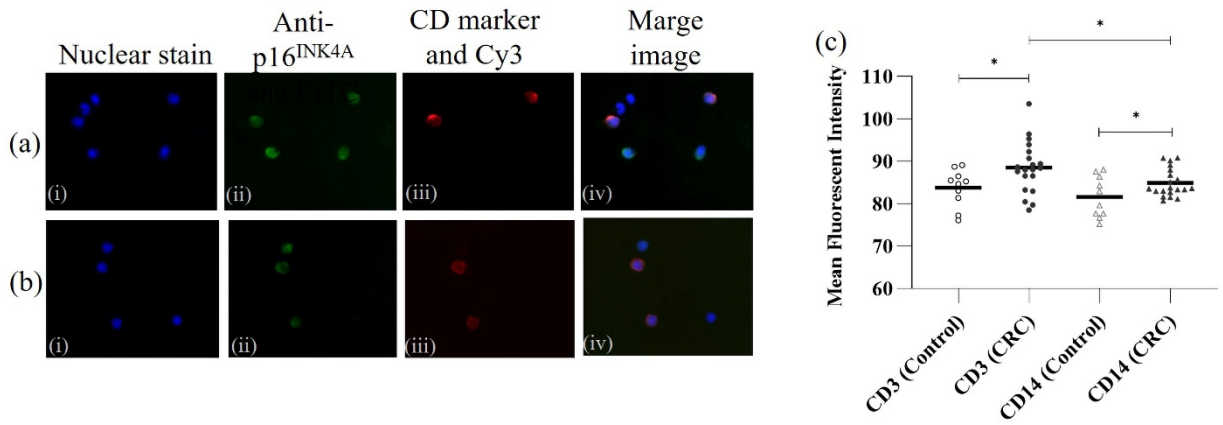
Nuclear stain
Anti-p16INK4A
CD marker and Cy3
Marge image
(a)
(b)
(i)
(ii)
(iii)
(iv)
(c)
Mean Fluorescent Intensity
110
100
90
80
70
60
*
*
*
CD3 (Control)
CD3 (CRC)
CD14 (Control)
CD14 (CRC)

Fig (5)

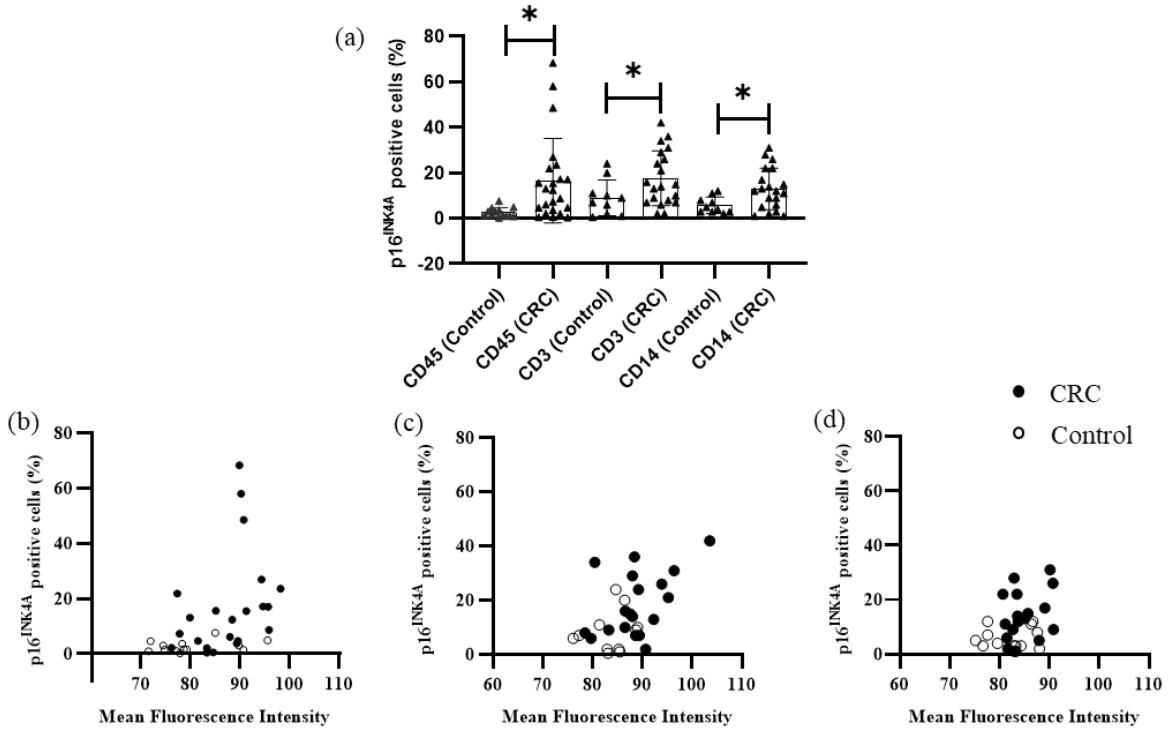
(a)
p16INK4A positive cells (%)
80
60
40
20
0
-20
*
*
*
CD45 (Control)
CD45 (CRC)
CD3 (Control)
CD3 (CRC)
CD14 (Control)
CD14 (CRC)
(b)
(c)
(d)
p16INK4A positive cells (%)
Mean Fluorescence Intensity
70
80
90
100
110
60
CRC
Control

Fig (6)

Fig (1) Immunofluorescence staining of $p16^{INK4A}$ antibodies in cell lines, **(a)** Hela cells with $p16^{INK4A}$ D7CM1 antibodies showing strong cytoplasmic staining, **(b)** Hela cells with $p16^{INK4A}$ D3W8G antibodies, **(c)** Rat epidermal keratinocytes with $p16^{INK4A}$ D7CM1 antibodies showing cytoplasmic staining, **(d)** Rat epidermal keratinocytes with $p16^{INK4A}$ D3W8G antibodies showing nuclear staining, **(e)** HCT116 with $p16^{INK4A}$ D7CM1 antibodies as negative control, **(f)** HCT116 with $p16^{INK4A}$ D3W8G antibodies as negative control

Fig (2) **(a)** Immunofluorescence staining of WBCs showing DAPI staining (i), $p16^{INK4A}$ staining (ii), CD45 staining (iii) and merged image (iv), the bar marker on the images represents 20μm, **(b)** Scatter plot of $p16^{INK4A}$ MFI of healthy controls and $p16^{INK4A}$ MFI of CRC group (age and sex adjusted cohort study), **(c)** Scatter plot of $p16^{INK4A}$ MFI of healthy controls and $p16^{INK4A}$ MFI of CRC group. The bar on the scatter plot represents mean value.

Fig (3) ROC analysis of $p16^{INK4A}$ in white blood cells of CRC patients and healthy controls. The Youden index point at the vertical solid line and horizontal solid line showing 78% sensitivity and 71% specificity.

Fig (4) Correlation of $p16^{INK4A}$ mean fluorescence intensity of CRC patients with clinical parameters. **(a)** Data from CRC patients were grouped according to age, **(b)** gender, **(c)** Clinical stages of CRC, (**d**) tumor sizes, (**e**) LN involvement and (**f**) metastasis or non-metastasis.

Fig (5) **(a)** Immunofluorescence staining of CD3+ peripheral immune cells showing DAPI staining (i), $p16^{INK4A}$ staining (ii), CD3 staining (iii) and merged image (iv), **(b)** Immunofluorescence staining of CD14+ peripheral immune cells showing DAPI staining (i), $p16^{INK4A}$ staining (ii), CD3 staining (iii) and merged image (iv), **(c)** Scatter plot of $p16^{INK4A}$ MFI

of healthy controls and $p16^{INK4A}$ MFI of CRC group in CD3+ and CD14+ cells. The bar on the scatter plot represents mean value.

Fig (6) **(a)** Comparison of $p16^{INK4A}$ positive cells in white blood cells, CD3+ cells and CD14+ cells between CRC group and healthy control group, **(b)** Correlation of $p16^{INK4A}$ positive cells percentage and $p16^{INK4A}$ mean fluorescent intensity of CRC patients and healthy controls in white blood cells, **(c)** Correlation of $p16^{INK4A}$ positive cells percentage and $p16^{INK4A}$ mean fluorescent intensity of CRC patients and healthy controls in CD3+ cells, **(d)** Correlation of $p16^{INK4A}$ positive cells percentage and $p16^{INK4A}$ mean fluorescent intensity of CRC patients and healthy controls in CD14+ cells.